УДК 531+620.17

С.А. Эпштейн, Е.Л. Коссович, М.Г. Минин, В.А. Просина

ОСОБЕННОСТИ ОБРАЗОВАНИЯ ТОНКОДИСПЕРСНЫХ ЧАСТИЦ ПРИ МЕХАНИЧЕСКИХ ИСПЫТАНИЯХ КАМЕННЫХ НИЗКОМЕТАМОРФИЗОВАННЫХ УГЛЕЙ НА НИЗКОРАЗМЕРНЫХ МАСШТАБНЫХ УРОВНЯХ

Аннотация. Исследованы особенности образования тонкодисперсных частиц при нагружении каменного низкометаморфизованного угля на микро- и наноуровнях. Для этого были использованы эксперименты по микро- и наноиндентированию. Исследование проводили на микрокомпоненте витрините, так как этот мацерал изменяет свои механические свойства в зависимости от вида и стадии метаморфизма углей. Величины модулей упругости, измеренные на микро- и наноразмерных уровнях, были сопоставимыми. Однако при измерении микро- и нанотвердости угля обнаружен размерный эффект, выражающийся в пропорциональном снижении величин твердости с увеличением приложенного нагружения. При экспериментах по циклическому наноиндентированию с увеличением максимальной нагрузки, приложенной к одной и той же области на поверхности угля, было обнаружено явление «деформационного упрочнения». Это явление заключается в быстром росте величин твердости и модулей упругости при циклическом индентировании с возрастающей максимальной нагрузкой. На основании ранее проведенных исследований механического поведения хрупких материалов, таких как керамика, и явлений разрушения углей при наноиндентировании, был сделан вывод о том, что вышеупомянутые эффекты (размерный эффект и «деформационное упрочнение») связаны с предрасположенностью структуры витринита к разрушению при нагружении на микро- и наноразмерных уровнях.

Ключевые слова: уголь, механические свойства, микротвердость, нанотвердость, модуль упругости, размерный эффект, разрушение.

DOI: 10.25018/0236-1493-2019-02-0-69-77

Introduction

Coal, up to the present, is an important resource for generating electricity and heat. Modern coal combustion plants are mainly based on technologies that use pulverized coal [1]. The efficiency of coal combustion in such technologies is largely determined by the particle size distribution (PSD) [1,2] and their reactivity [3]. The particle size distribution during fine grinding of coal is largely determined by the physicomechanical properties of coals and the characteristics reflecting the strength of the inter- and supramolecular interactions in the coal structure. As the physico-mechanical characteristics, the following indices are estimated, such as Hardgrove grindability test [4,5], wearing capacity [6], hardness [7], etc. Tightly bound with these characteristics, there exist other indices such as elastic moduli, Poisson's ratio and maximum strength.

ISSN 0236-1493. Горный информационно-аналитический бюллетень. 2019. № 2. С. 69–77.

Such parameters are usually found by the large-scale tests, such as uniaxial [8—10] or triaxial [9,11,12] compression, tension [13,14], bending [15], cutting [16] and microhardness (Vickers) indentation [7,17,18]. Unfortunately, most of the listed methods do not allow for characterization of coals ability to form fine particles of the known class of sizes. This happens due to the high heterogeneity of coals at micro- and even nanoscale [15]. Recently it was established that it is difficult to obtain the repeatable results even at microscale due to the differences between mechanical properties of different coal macerals [17]. Overcome of these issues was sought and found in application of the depth-sensing nanoindentation technique at individual coal macerals. First works were made at the transparent thin sections of coals. The procedure was of depth-sensing indentation with determination of the appropriate area of indentation occupied by the individual maceral by transmitted light microscopy (see [19]). There, it was established that all the coal macerals are available for obtaining their mechanical properties by nanoindentation, whereas microindentation is applicable to only a few of them, namely, vitrinite and, partially, inertinite (when its macerals have appropriate sizes of several tens of microns). In [20] and, independently, in [21], results on depth-sensing microindentation at different coal macerals were discussed aimed at determination of the differences between the vitrinite and inertinite mechanical properties for coals of different type and rank. More advanced procedures of micro- and nanoindentation results interpretation at coals microcomponents were shown in [22—24].

Despite the efficiency of depth-sensing micro- and nanoindentation techniques application for studying of coals mechanical properties and their heterogeneity with respect to maceral composition, there exist many questions related to the results that are being obtained. For example, in [25], authors argued that coals matter is rather brittle and, under the indentation impact, it crushes into the fine powder. The sizes of such particles are much smaller than the size of the resulting imprint, that is, for nanoindentation, of two to five microns diameter. This effect, to the belief of the authors of the current article, might tightly connected with coals behaviour at crushing during preparation of pulverized fuel. If the specific coal tends to form very fine particles during indentation, it is supposed to form them at crushing, therefore making it less valuable for pulverized fuel preparation.

In the current article, the low-rank hard coal mechanical behavior (at low-dimensional scales) was studied with respect to structural changes leading to crushing under the forces applied to the indenter. To this end, different types of indentation techniques were used, including depth-sensing micro- and nanoindentation, microhardness measurement and cyclic loading.

Materials and methods

Samples preparation and description

In this work we concentrated on coal aimed at energy production. The selected low-rank hard coal (vitrinite reflectance index $R_{o,r}$ = 0.65%Vol.) has relatively low Carbon contents (80.19%) and consists of 70% of vitrinite macerals group. Such high vitrinite contents allows for preparation of rather wide range of samples for indentation at different scales (micro and nano) satisfying the requirements for obtaining the reliable results [24]. All the subsequent mechanical tests were performed at vitrinite microcomponents as they represent the special features of coals at low scale, such as sensitivity to the rank and type [21,24,26].

According to the previously constructed technique [21], samples were prepared

shaped as sections of coals with polished smooth surface perpendicular to the bedding direction. Samples were manufactured from fragments of coal whose thickness was not smaller than 20—30 mm. No binders or cementing admixtures, or mechanical compaction were involved at any stage of preparation. The samples surfaces were smoothed and polished using polishing machine RotoPol-35 (Struers, Demark). Final smoothing (polishing) was carried out with glycerine instead of water. The resultant samples had comparable dimension with the sizes of the initial fragments, with height of 10—25 mm.

Indentation techniques

Depth-sensing indentation (DSI) techniques were introduced by Kalei [27]. If the depth of indentation is below micrometer scale, then the term depth-sensing nanoindentation (DSNI) is used. As a part of DSI, the load-displacement (*P-h*) diagram is continuously monitored for load increase and decrease, where, *h* is the depth of indentation (penetration of the indenter into the sample surface) and *P* is the force applied to the indenter. Typical *P-h* curves for metals and many materials have usually two branches that do not coincide because the curve reflects both elastic and plastic deformation of the material at the loading, while the unloading of metals occurs usually elastically. In 1975 the Bulychev-Alekhin-Shorshorov relation (BASh) relation was derived [28]

$$S = dP / dh = 2E^* a \approx 2E^* \sqrt{A / \pi}, \quad (1)$$

where *S* is the inclination of the displacement-load curve, *a* is the characteristic size of the contact zone. *A* is the area of the contact and E^* is the contact elastic modulus. Within the framework of the Hertz contact theory, E^* is determined as a combination of elastic moduli E_i and E_s and Poisson's ratios ν_i and ν_s for indenter (with index *i*) and sample (index *s*):

$$\frac{1}{E^*} = \frac{1-\nu_i^2}{E_i} + \frac{1-\nu_s^2}{E_s}. \quad (2)$$

Thus, the basic relations for determination of the sample elastic modulus E_s and hardness *HM* are as follows:

$$E_s = \left(1 - \frac{E^*}{E_i^*}\right)^{-1} \left(1-\nu_s^2\right) E^*, \quad (3)$$

where $E_i^* = \frac{E_i}{1-\nu_i}$ is the reduced elastic contact modulus of the indenter;

$$HM = \frac{P_{max}}{A}, \quad (4)$$

where P_{max} is the peak force applied to the surface by indenter.

The BASh relation (1) accompanied by additional assumptions allow calculation of local values of the reduced elastic contact modulus and hardness of the sample using Oliver-Pharr [29] approach.

During the last few decades, the Oliver and Pharr (OP) approach for evaluation of elastic moduli and hardness of materials [29,30] is generally included into the DSNI equipment software. The OP technique is based on the use of experimental values of the maximum load P_{max}, the corresponding maximum approach h_{max} of the indenter and sample, and values of the elastic stiffness *S*, measured for the unloading branch of the *P-h* curve at $P = P_{max}$ and $h = h_{max}$.

Instrumented tests were performed at two different DSI facilities: nanotriboindenter Hysitron TI750 UBI with Berkovich indenter and MicroHardness Tester (CSM Instruments, Switzerland) with Vickers indenter. The latter allows tests at relatively higher peak loads (up to 1000 mN), whereas the P_{max} of the former device is limited to 12 mN (or 12 000 μN). Additionally, hardness measurements were performed at PMT-3 microhardness tester (LOMO, Russia). It is worth to note that the PMT-3 device does not provide the continuous

monitoring of the load-displacement (*P-h*) curve but rather allowed us to measure the hardness after the unloading of the sample. Hence, the microhardness tests are referred to as static microindentation tests. Microhardness was determined according to the standard procedures [7,31] on the basis of evaluation of the imprint diagonals sizes. The essence of the method consists in measuring the length of a diagonal of a square imprint remaining on the surface of the sample after pressing the Vickers diamond pyramid under constant load.

Experiments at Hysitron TI750 UBI were done by load-control mode with trapezoidal protocol (two seconds hold at peak load). At the zone occupied by vitrinite maceral, a square 70x70 μm area was chosen and series of DSNI measurements (not less than 36 indents) were implemented within this area. Tests at MicroHardness Tester were also done using load-control mode with trapezoidal protocol with 15 s hold at maximum load. Microhardness measurements at PMT-3 were done with 10 s hold at load.

For indentations of the vitrinite maceral domains of the considered coal, the peak load P_{max} were as follows: 4000 μN for DSNI, 500 mN for DSI by the microindenter, and 200, 500 and 1000 mN for microhardness measurements. At each sample, not less than 15 indentations were performed for the vitrinite maceral domains.

In addition, experiments were performed on cyclic loading of samples. Such studies allow us to characterize the strength and wear resistance (tendency to fracture) of materials under repeated loads. For carrying out experiments on nanoindentation, at least four points were selected and, sequentially, a sample of coal or anthracite with a maximum load in the range of 10—10,000 μH was loaded and unloaded 12 times in each of the selected points. *P-h* diagrams were obtained. The range of changes in the measured values of the modulus of elasticity and nanohardness was characterized.

Values of the measured diagonals of the imprints at different loads

P_{max}, mN	$d_{average}$, μm
200	30.0±0.2
500	50.0±1.0
1000	78.0±0.5

Results and discussion

The hardness measurements of the vitrinite maceral of the considered coal revealed the drastic increase of the resulting measured imprints diagonals ($d_{average}$) with load growth, as shown in Table. It could be seen that the size of the diagonals grows drastically with the peak force increase.

The shape of the imprints was visibly plastic, with some cracks within the contact area between coal and indenter, and just in case when P_{max} = 1000 mN, it was found a crack coming out of the edge of one diagonal.

To evaluate the elastic contact modulus, one needs to analyze the experimental load-displacement curves. Figure 1 demonstrates the typical shapes of *P-h* curves obtained at nano- and microindentation of the considered coal. As it has been observed for other coals [24], the shapes of load-displacement diagrams obtained after nano- and microindentation are qualitatively similar.

To characterize such a similarity quantitatively, we use a parameter (R_W, %) that is the ratio between the hysteresis loop (A_{hys}) to the full work of indenter tip at loading of the sample (A_{load}). Therefore, parameter R_W is calculated as follows:

$$R_W = \frac{A_{hys}}{A_{load}} \cdot 100\%. \qquad (5)$$

A scheme explaining the meaning of A_{hys} and A_{load} works was presented in [24].

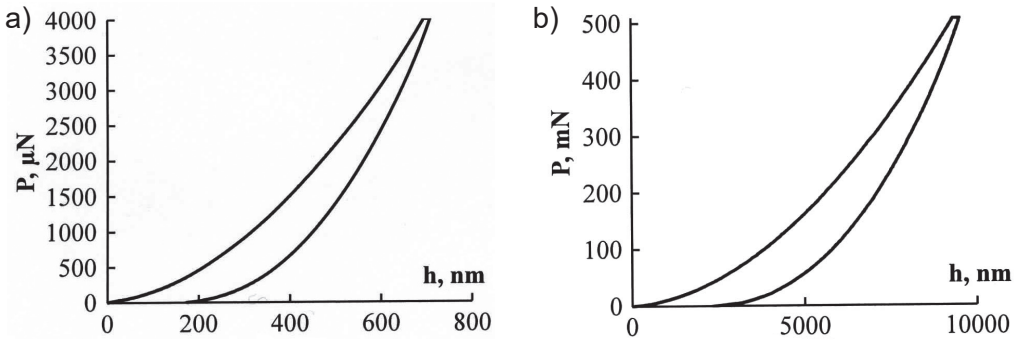

Fig. 1. Typical load-displacement curves obtained for the low-rank bituminous coal, vitrinite maceral, at (a) nano- ; and (b) micro scales of indentation

The average values of R_W for the considered coal at nanoindentation were R_W = = 34.2±1.5%, whereas at microindentation R_W = 36.0±2.0%, and these could be considered as similar for both nano and microscales of tests.

Nanoindentation measurements allowed to obtain the following value of the coal elastic modulus E_s = 3.60±0.08% GPa. For depth-sensing microindentation, E_s = = 3.62±0.07% GPa. It could be seen that the values of elastic moduli measured at different scales of indentation are very similar.

On the other hand, the hardness values decrease with growth of the peak load, as shown in Figure 2. An unexpectedly fast decay of hardness values with the increase of the peak load acting on the indenter could be observed.

Actually, the hardness tests demonstrated rather unpredictable scaling effects. Indeed, one could expect that the values of hardness obtained in static experiments by the microhardness device should be higher than the values obtained in DSNI tests because the area used in (4) is the elastically recovered area of the imprint after full unloading, while one uses in a DSNI test the area of the contact region under maximum load. However, here we obtained the opposite result. Moreover, there coul be observed a linear decay of the hardness values with the peak

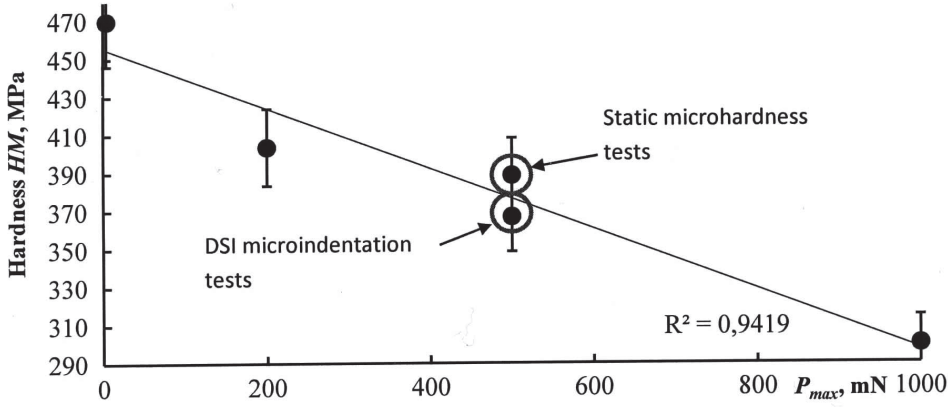

Fig. 2. Scaling effects of the hardness values for the vitrinite of low-rank bituminous coal. The hardness values are calculated according to depth-sensing indentation and microhardness measurement. Vertical lines determine standard deviation of the measured values

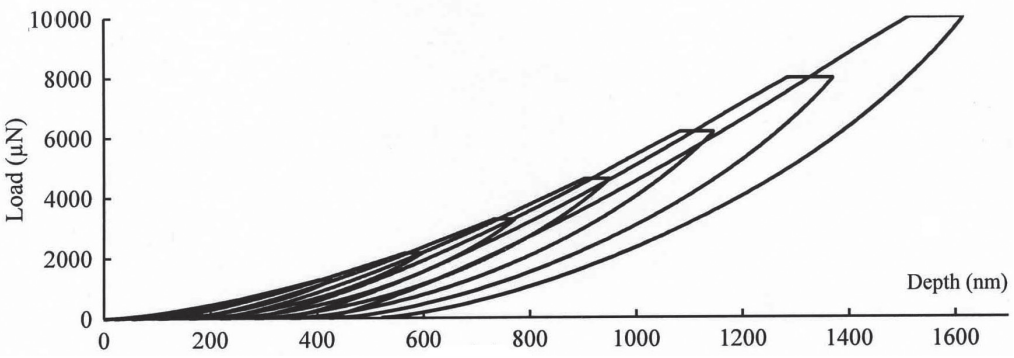

Fig. 3. Typical P-h diagram for the low-rank hard coal obtained by the cyclic loading

force growth (including from nano- to microscales). Such an effect is rather not typical, as for most of the materials, there exist only a logarithmic decay of hardness [32,33].

Cyclic loading by the nanoindenter allowed for the following results. Figure 3 demonstrates the typical *P-h* curves obtained at low-rank bituminous coal after a series of indentation at the single point with increasing maximal load from cycle to cycle. It could be seen that, according to the changes in the *P-h* curves from cycle to cycle, the coal matter in this case is being changed drastically. This could be proved by the increase of the yield plateau, visible increase of the hysteresis and intersections between the curves, that is typical for the materials with granulated structure with low interconnections between elements [34].

The measured values of hardness and elastic moduli during the indentation at each cycle have shown a drastic increase: HM grew between 404 to 502 MPa, Es — from 4.40 to 5.17 GPa. This indicates the 'strain hardening' effect, that is typical to the materials with rather homogenous structure and tendency to plastic behavior. It is worth to be mentioned that the visible 'plasticity' of low-rank hard coal behavior at microindentation is not the real plasticity in terms of metals behavior due to the natural brittleness of coals and lack of their integrity at microscale (presence of cracks, pores, heterogeneity, etc.). It is rather natural to assume that such 'strain-hardening' effect is tightly connected with the hardness values decay along with the growth of the scale of indentation tests (i.e. increase of maximal force). The latter is not typical for the materials that maintain their integrity during indentation tests, but is relatively widely found for brittle and ductile materials such as ceramics [35,36]. For brittle materials, the scaling effect and 'strain hardening' are related to loss of integrity of the initially bulk surface under acting of the indenter [36,37]. This makes the error of measuring of hardness due to the fact that now hardness is being found for a 'powder' that was formed by crushing of the sample in the contact with the indenter. For the first time, similar coals matter behavior (crushing) was discussed in [25], where this effect was described by theoretical asymptotic analysis of the experimental data. In the view of above, one may see that the effects that were observed during micro- and nanoindentation tests of low-rank hard coal are reasoned by the fact that its surface is being crushed into the fine powder in the contact area with the indenter.

Conclusions

In the current paper, a low-rank hard coal was studied in order to characterize

its propensity to formation of fine particles under vertical loading. To this end, micro- and nanoindentation were used. The vitrinite microcomponents of the selected coal were investigated due to their special features (including previously established variations in their mechanical properties with coal rank and type).

The scaling effects were observed during measuring of its micro- and nanohardness values, namely, the hardness linear decrease with growth of applied force (and subsequent increase of the contact area with the indenter).

The effect of 'strain hardening' was found during repeatable (cyclic) nanoindentation with the increasing maximal load to the same area at the coal surface. This effect consists of rapid growth of hardness and elastic moduli values during repeatable indentation along with the increase of the applied maximal force.

In the view of the previous investigations on mechanical behavior of brittle materials such as ceramics, and with the theoretically found observations on coals crushing during indentation, it was concluded that the aforementioned effects (scaling and 'strain hardening') are connected with the propensity of loss of the vitrinite structure integrity under vertically applied loads (at micro- and nanoscales).

КОРОТКО ОБ АВТОРАХ

Эпштейн Светлана Абрамовна[1] — доктор технических наук,
старший научный сотрудник, зав. лабораторией,
e-mail: apshtein@yandex.ru,
Коссович Елена Леонидовна[1] — кандидат физико-математических наук,
старший научный сотрудник, e-mail: e.kossovich@misis.ru,
Минин Максим Геннадьевич — младший научный сотрудник,
Физико-технологический институт, Уральский федеральный университет,
Просина Вера Алексеевна[1] — студент, лаборант,
[1] НИТУ «МИСиС».

ISSN 0236-1493. Gornyy informatsionno-analiticheskiy byulleten'. 2019. No. 2, pp. 69–77.

Insights into fine particles formation by low-rank hard coals mechanical testing at low dimensional scales

Epshtein S.A.[1], Doctor of Technical Sciences, Head of Laboratory,
Senior Researcher, e-mail: apshtein@yandex.ru,
Kossovich E.L.[1], Candidate of Physical and Mathematical Sciences,
Senior Researcher, e-mail: e.kossovich@misis.ru,
Minin M.G., Junior Researcher, Institute of Physics and Technology,
Ural Federal University, 620002, Ekaterinburg, Russia,
Prosina V.A.[1], Student, Laboratory Assistant,
1 National University of Science and Technology «MISiS»,
119049, Moscow, Russia.

Abstract. Low-rank hard coal was studied in order to characterize its propensity to formation of fine particles under vertically applied loading at micro- and nanoscales. To this end, micro- and nanoindentation tests were used. The vitrinite microcomponents of the selected coal were investigated due to their variations in mechanical properties with coal rank and type. Values of elastic moduli measured at micro- and nanoscales were similar. On the other hand, the scaling effects were observed during measuring of low-rank hard coal micro- and nanohardness, namely, the hardness linear decrease with growth of applied force. The effect of 'strain hardening' was found during repeatable (cyclic) nanoindentation with the increasing of the maximal load applied to the same area at the coal surface. This effect consists of rapid

growth of hardness and elastic moduli values during repeatable indentation along with the increase of the applied maximal force. In the view of the previous investigations on mechanical behavior of brittle materials such as ceramics, and with the observations on coals crushing during nanoindentation, it was concluded that the aforementioned effects (scaling and 'strain hardening') are connected with the propensity of loss of the vitrinite structure integrity under vertically applied loads (at micro- and nanoscales).

Key words: coal, mechanical properties, microhardness, nanohardness, elastic modulus, scaling effect, crushing.

DOI: 10.25018/0236-1493-2019-02-0-69-77

ACKNOWLEDGEMENTS

Authors thank the Russian Science Foundation (grant #18-77-10052) for financial support of this work.

REFERENCES

1. Ganguli R., Bandopadhyay S. Relationship between particle size distribution of low-rank pulverized coal and power plant performance. *Journal of Combustion*, 2012. Vol. 2012, No di. DOI: 10.1155/2012/786920.

2. Liu Y., Lu H., Guo X., Gong X., Sun X., Zhao W. An investigation of the effect of particle size on discharge behavior of pulverized coal. *Powder Technology*, 2015. Vol. 284. Pp. 47—56. DOI: 10.1016/j.powtec.2015.06.041.

3. Li Q., Zhao C., Chen X., Wu W., Li Y. Comparison of pulverized coal combustion in air and in O2/CO2 mixtures by thermo-gravimetric analysis. *Journal of Analytical and Applied Pyrolysis*, 2009. Vol. 85, No 1—2. Pp. 521—528. DOI: 10.1016/j.jaap.2008.10.018.

4. Hower J.C., Graese A.M., Klapheke J.G. Influence of microlithotype composition on hardgrove grindability for selected eastern Kentucky coals. *International Journal of Coal Geology*, 1987. Vol. 7, No 3. Pp. 227—244. DOI: 10.1016/0166—5162(87)90038-3.

5. Tichánek F. Contribution To Determination of Coal Grindability Using Hardgrove Method *Příspěvek Ke Stanovení Melitelnosti Uhlí Metodou*. 2008. Vol. LIV, No 1. Pp. 27—32.

6. Amdur A.M., Zagainov S.A., Raznitsina A.L. Strength characteristics of coals - substitutes of coke in metallurgical aggregates. News of the Higher Institutions. *Mining Journal*, 2012. No. 2. Pp. 192—196.

7. *GOST 21206-75 Coals and anthracite. Determination method for microhardness and microbrittleness*. 1977. Russian p.

8. Zhao Z., Wang W., Dai C., Yan J. Failure characteristics of three-body model composed of rock and coal with different strength and stiffness. Transactions of Nonferrous Metals Society of China, 2014. Vol. 24, No 5. Pp. 1538—1546. DOI: 10.1016/S1003-6326(14)63223-4.

9. Shkuratnik V.L., Nikolenko Pp. V., Koshelev A.E. Stress dependence of elastic P-wave velocity and amplitude in coal specimens under varied loading conditions. *Journal of Mining Science*, 2016. Vol. 52, No 5. Pp. 873—877. DOI: 10.1134/S1062739116041322.

10. Pan J., Meng Z., Hou Q., Ju Y., Cao Y. Coal strength and Young's modulus related to coal rank, compressional velocity and maceral composition. *Journal of Structural Geology*, 2013. Vol. 54. Pp. 129—135. DOI: 10.1016/j.jsg.2013.07.008.

11. Shkuratnik V.L., Filimonov Y.L., Kuchurin S. V. Regularities of Acoustic Emission in Coal Samples under Triaxial Compression. *Journal of Mining Science*, 2005. Vol. 41, No 1. Pp. 44—52. DOI: 10.1007/s10913-005-0062-8.

12. Shkuratnik V.L., Filimonov Y.L., Kuchurin S. V. Acoustic-emissive memory effect in coal samples under triaxial axial-symmetric compression. *Journal of Mining Science*, 2006. Vol. 42, No 3. Pp. 203—209. DOI: 10.1007/s10913-006-0048-1.

13. Zhao Y., Liu S., Jiang Y., Wang K., Huang Y. Dynamic Tensile Strength of Coal under Dry and Saturated Conditions. *Rock Mechanics and Rock Engineering*, 2016. Vol. 49, No 5. Pp. 1709—1720. DOI: 10.1007/s00603-015-0849-0.

14. Zhao Y., Zhao G.-F., Jiang Y., Elsworth D., Huang Y. Effects of bedding on the dynamic indirect tensile strength of coal: Laboratory experiments and numerical simulation. *International Journal of Coal Geology*, 2014. Vol. 132. Pp. 81—93. DOI: 10.1016/j.coal.2014.08.007.

15. West R.D., Markevicius G., Malhotra V.M., Hofer S. Variations in the mechanical behavior of Illinois bituminous coals. *Fuel*, 2012. Vol. 98. Pp. 213—217. DOI: 10.1016/j.fuel.2012.03.042.

16. Korshunov A.N., Dergunov D.M., Logov A.B., Gerike B.L. Coal cutting with a disk. *Soviet Mining Science*, 1975. Vol. 11, No 5. Pp. 571—573. DOI: 10.1007/BF02499387.

17. Macmillan N.H., Rickerby D.G. On the measurement of hardness in coal. *Journal of Materials Science*, 1979. Vol. 14, No 1. Pp. 242—246. DOI: 10.1007/BF01028354.

18. Das B. The effect of load on Vicker's indentation hardness of coal. *International Journal of Rock Mechanics and Mining Sciences*, 1972. Vol. 9, No 6. Pp. 783—788. DOI: 10.1016/0148-9062(72)90036-8.

19. Borodich F.M., Bull S.J., Epshtein S.A. Nanoindentation in Studying Mechanical Properties of Heterogeneous Materials. *Journal of Mining Science*, 2015. Vol. 51, No 3. Pp. 1062—7391. DOI: 10.1134/S1062739115030072.

20. Kožušníková A. Determination of Microhardness and Elastic Modulus of Coal Components by Using Indentation Method. *GeoLines*, 2009. Vol. 22. Pp. 40—43.

21. Kossovich E.L., Dobryakova N.N., Epshtein S.A., Belov D.S. Mechanical properties of coal microcomponents under continuous indentation. *Journal of Mining Science*, 2016. Vol. 52, No 5. Pp. 906—912. DOI: 10.1134/S1062739116041382.

22. Epshtein S.A., Borodich F.M., Bull S.J. Evaluation of elastic modulus and hardness of highly inhomogeneous materials by nanoindentation. Applied Physics A: *Materials Science and Processing*, 2015. Vol. 119, No 1. Pp. 325—335. DOI: 10.1007/s00339-014-8971-5.

23. Kossovich E.L., Borodich F.M., Bull S.J., Epshtein S.A. Substrate effects and evaluation of elastic moduli of components of inhomogeneous films by nanoindentation. *Thin Solid Films*, 2016. Vol. 619. Pp. 112—119. DOI: 10.1016/j.tsf.2016.11.018.

24. Kossovich E.L., Epshtein S.A., Shkuratnik V.L., Minin M.G. Perspectives and problems of modern depth-sensing indentation techniques application for diagnostics of coals mechanical properties. *Gornyy Zhurnal*, 2017. No 12. Pp. 25—30. DOI: 10.17580/gzh.2017.12.05.

25. Argatov I.I., Borodich F.M., Epshtein S.A., Kossovich E.L. Contact stiffness depth-sensing indentation: Understanding of material properties of thin films attached to substrates. *Mechanics of Materials*, 2017. Vol. 114. Pp. 172—179. DOI: 10.1016/j.mechmat.2017.08.009.

26. Kossovich E., Epshtein S.A., Dobryakova N., Minin M., Gavrilova D. Mechanical Properties of Thin Films of Coals by Nanoindentation. *Physical and Mathematical Modeling of Processes in Geomedia: 3d International Scientific School of Young Scientists*; November 01—03, 2017, Moscow: IPMech RAS, 2018. Pp. 45—50. DOI: 10.1007/978-3-319-77788-7_6.

27. Kalei G.N. Some results of microhardness test using the depth of impression. *Mashinovedenie*, 1968. Vol. 4, No 3. Pp. 105—107.

28. Bulychev S.I., Alekhin V.P., Shorshorov M.K., Ternovskij A.P., Shnyrev G.D. Determination of Young modulus by the hardness indentation diagram. *Zavodskaya Laboratoriya*, 1975. Vol. 41, No 9. Pp. 1137—1140.

29. Oliver W.C., Pharr G.M. An improved technique for determining hardness and elastic modulus using load and displacement sensing indentation experiments. *Journal of Materials Research*, 1992. Vol. 7, No 06. Pp. 1564—1583. DOI: 10.1557/JMR.1992.1564.

30. Oliver W.C., Pharr G.M. Measurement of hardness and elastic modulus by instrumented indentation: Advances in understanding and refinements to methodology. *Journal of Materials Research*, 2004. Vol. 19, No 01. Pp. 3—20. DOI: 10.1557/jmr.2004.19.1.3.

31. *ASTM. ASTM E384: Standard Test Method for Microindentation Hardness of Materials*. Annual Book of ASTM Standards 2016. 1—42 Pp. DOI: 10.1520/E0384-10.2.

32. Halgaš R., Dusza J., Kaiferová J., Kovácsová L., Markovská N. Nanoindentation testing of human enamel and dentin. *Ceramics — Silikaty*, 2013. Vol. 57, No 2. Pp. 92—99.

33. Dutta A.K., Narasaiah N., Chattopadhyaya A.B., Ray K.K. The load dependence of hardness in alumina-silver composites. *Ceramics International*, 2001. Vol. 27, No 4. Pp. 407—413. DOI: 10.1016/S0272-8842(00)00095-X.

34. Faisal N.H., Prathuru A.K., Goel S., Ahmed R., Droubi M.G., Beake B.D., Fu Y.Q. Cyclic Nanoindentation and Nano-Impact Fatigue Mechanisms of Functionally Graded TiN/TiNi Film. *Shape Memory and Superelasticity*, 2017. Vol. 3, No 2. Pp. 149—167. DOI: 10.1007/s40830-017-0099-y.

35. Menčík J., Elstner M. Indentation Size Effects in Ductile and Brittle Materials. *Key Engineering Materials*, 2013. Vol. 586. Pp. 51—54. DOI: 10.4028/www.scientific.net/KEM.586.51.

36. Voyiadjis G., Yaghoobi M. Review of Nanoindentation Size Effect: Experiments and Atomistic Simulation. *Crystals*, 2017. Vol. 7, No 10. Pp. 321. DOI: 10.3390/cryst7100321.

37. Samadi-Dooki A., Voyiadjis G.Z., Stout R.W. A combined experimental, modeling, and computational approach to interpret the viscoelastic response of the white matter brain tissue during indentation. *Journal of the Mechanical Behavior of Biomedical Materials*, 2017. Vol. 77. Pp. 24—33. DOI: 10.1016/j.jmbbm.2017.08.037. ГИАБ .